

# High resolution inelastic x-ray scattering spectrometer at the advanced photon source

M. Schwoerer-Böhning,<sup>a)</sup> A. T. Macrander, and P. M. Abbamonte

Argonne National Laboratory, Advanced Photon Source, Experimental Facilities Division, Argonne, Illinois 60439

D. A. Arms

Department of Physics and Frederick Seitz Materials Research Laboratory, University of Illinois at Urbana-Champaign, Urbana, Illinois 61801

(Received 20 April 1998; accepted for publication 24 June 1998)

We have commissioned a new instrument for high resolution inelastic x-ray scattering on the inelastic scattering beamline of the Synchrotron Radiation Instrumentation Collaborative Access Team on sector 3 of the Advanced Photon Source. So far, the instrument is set up at 13.84 keV with a total energy resolution of 7.5 meV and a momentum resolution of  $\leq 0.1 \text{ \AA}^{-1}$ . We present technical details of the instrument, which includes an in-line monochromator, a focusing mirror, and a focusing analyzer. The performance of the instrument was demonstrated in studies of phonons in diamond and chromium. © 1998 American Institute of Physics. [S0034-6748(98)04109-4]

## I. INTRODUCTION

Inelastic x-ray scattering experiments with a resolution sufficient to study phonons is a new field that has arisen due to the availability of synchrotron radiation.<sup>1</sup> The very low scattering cross section and the narrow bandpass needed (of the order of  $\Delta E/E = 10^{-7}$ ) require x-ray sources of high brilliance. The pioneering instrument for high resolution inelastic x-ray scattering (HRIXS) called INELAX developed by Burkel, Dorner, and Peisl at the Hamburger Synchrotronstrahlungs Labor (HASYLAB)<sup>2,3</sup> is not installed at such a high brilliance source. INELAX and the more recent instrument at the European Synchrotron Radiation Facility (ESRF)<sup>4</sup> follow a backscattering geometry for their monochromators to achieve the narrow incident bandpass. The advantage of using backscattering geometry in x-ray diffraction (an optical arrangement originally used in inelastic neutron scattering experiments<sup>5</sup>) was demonstrated by Sykora, Peisl, Graeff, and Materlik.<sup>6,7</sup> A backscattering monochromator as used at the ESRF and at HASYLAB limits the space near the sample because the premonochromatized beam must pass close to the sample. Thus, there is not enough room for large size sample containments (cryostats, high pressure cells). Energy scanning with a backscattering monochromator is achieved by tuning the temperature difference between the monochromator and a high resolution analyzer. Such measurements of energy transfers require a continuous scanning of the crystal temperature. The large energy transfers needed to study optical phonons ( $\Delta E \approx 100$  meV) take long scan times (400 steps with a stepsize of 0.25 meV) where difficulties in ascertaining the zero of the energy arise. The inelastic scattering beamline in the Synchrotron Radiation Instrumentation Collaborative Access Team (SRI-CAT) of the Advanced Photon Source (APS) has instead employed angle-tuned in-line monochromators to set a narrow

bandpass.<sup>8,9</sup> Changing the energy from an elastic peak to the desired phonon peak is no longer time consuming. The high resolution monochromator follows a mirror, which focuses the x-ray beam horizontally and vertically onto the sample position of a five-circle diffractometer. A focal size of ca.  $0.5 \times 0.5 \text{ mm}^2$  can be achieved. The horizontal focal length is fixed due to a fixed sagittal curvature of the mirror. A vertical bending mechanism can focus the beam at different locations downstream. The photon flux at the sample position ranges between 3 and  $5 \times 10^9$  photons/s in a 5 meV bandpass. On the five-circle diffractometer, a high resolution backscattering analyzer is mounted at a distance of 2.7 m. A schematic layout of the beamline is shown in Fig. 1.

## II. MONOCHROMATORS

The primary high heat load (HHL) monochromator is a double-crystal monochromator in ( $\pm$ ) configuration. It consists of two diamond crystals employing (111) reflections. The first crystal, which is exposed to the total radiation power emitted by the undulator insertion device, is water-cooled. Details concerning the performance of the water-cooled diamond crystal are described elsewhere.<sup>10,11</sup> A high resolution monochromator limits the bandpass of the monochromatic photons from the HHL monochromator to 5.2 meV at 13.84 keV.<sup>12</sup> Its design and performance have already been detailed by Macrander *et al.*<sup>13</sup> The four-reflection monochromator with one channel-cut crystal nested inside another uses asymmetric silicon (422) and (884) reflections (Fig. 2). Tuning of the incident energy is performed by rotating the inner crystal. A scan range of a few electron volt is achievable.

## III. HIGH RESOLUTION FOCUSING ANALYZER

Perfect crystals are required to achieve an energy resolution approaching the intrinsic Darwin width. The current

<sup>a)</sup>Electronic mail address: schwoere@aps.anl.gov

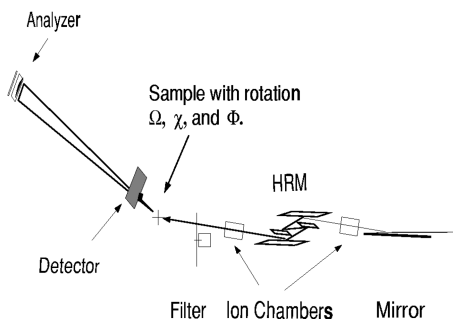


FIG. 1. Instrument layout at the APS (HRM=high resolution monochromator).

setup uses silicon wafers obtained from Virginia Semiconductors. Strain due to bending broadens the width of their reflections. Various methods have been developed to solve this problem.<sup>1,14</sup>

The contributions to the energy resolution of an analyzer separate into two major terms, the intrinsic and the geometric:

$$\left(\frac{dE}{E}\right)^2 = \left(\frac{dE_\tau}{E}\right)^2 + \left(\frac{dE_g}{E}\right)^2. \quad (1)$$

The intrinsic term  $dE_\tau$  ( $\tau$  denotes a particular x-ray reflection) of the energy resolution is mainly given by the Darwin width of the reflection used. In the case of propagating strain in the crystal, the intrinsic width is strain broadened. The geometric term  $dE_g$  considers the divergence  $\Delta\varepsilon$  of the scattered beam at nonzero deviation from backscattering ( $\varepsilon = \pi - \theta$ ) (Fig. 3). Usually the detector sits very close to the sample to keep  $\varepsilon$  small. Thus, there are always contributions due to the geometric term. The contributions to the total energy resolution do not necessarily add as do Gaussian distributions, but for our purpose it is a good approximation.<sup>15</sup>

To avoid strain broadening in the bent crystal, Dorner *et al.*<sup>2</sup> had the silicon wafers diced into a pattern of  $0.8 \times 0.8 \text{ mm}^2$  blocks. The blocks were kept oriented by leaving a  $200 \text{ }\mu\text{m}$ -thick backwall. Nevertheless, this kind of prepared wafer still shows significant strain propagating from the bent backwall into the remaining blocks. Furthermore, the reflected x-rays also probe the severely strained backwall exposed by the grooves. The current work was motivated by the need to relieve the residual strain and avoid scattering from within the grooves.

The new approach is a silicon wafer bonded to a glass wafer using epoxy. After dicing through the silicon into the glass, a backwall is left in the glass only. A detailed descrip-

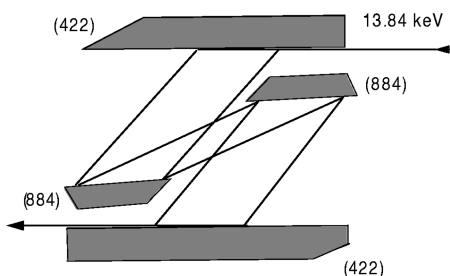


FIG. 2. The high resolution monochromator.

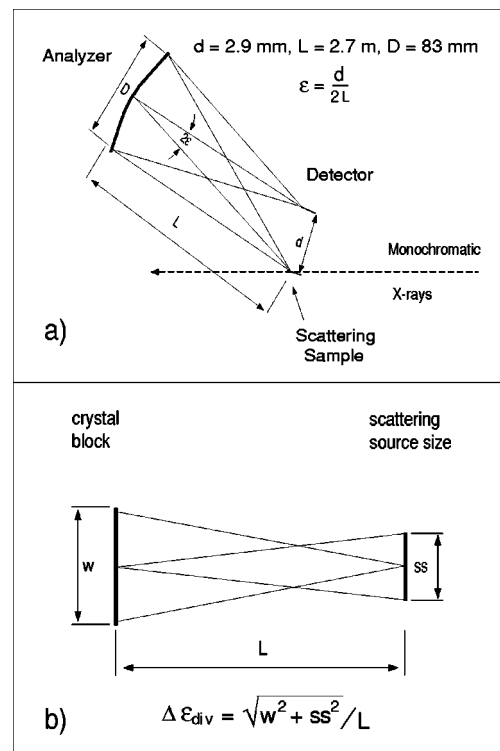


FIG. 3. Backscattering setup for HRIXS:  $L$ =analyzer-to-sample distance ( $L >$  Rowland circle),  $D$ =analyzer diameter, and  $d$ =image-to-scattering-source distance.

tion of fabricating such a ‘‘sandwich’’ analyzer is given elsewhere.<sup>16</sup> So far, analyzers have been made for bending radii of 2.6 and 1 m, with the latter one intended for medium energy resolution (a few 100 meV). The propagating strain from the backwall is reduced because glass is softer than silicon. Furthermore, the strained glass backwall does not contribute to the scattering.

We note that the magnitude of the intrinsic term depends on the material and on the order of the back reflection used. High energy resolution ( $\sim 1 \text{ meV}$ ) requires high order reflections, i.e., high energy x-rays ( $> 20 \text{ keV}$ ). At these high energies, the penetration of the x-rays can exceed a few millimeters, in which case the x-rays become even more sensitive to strain.

The geometric term to second order is given by

$$\frac{dE_g}{E} = \tan(\varepsilon)\Delta\varepsilon + \frac{(\Delta\varepsilon)^2}{2\cos^2(\varepsilon)}. \quad (2)$$

One can see that the magnitude of the geometric contribution mainly scales with  $\varepsilon$ . The divergence  $\Delta\varepsilon$  is given by a convolution of contributions due to the source size (scattering volume) and the block sizes of the analyzer [Fig. 3(b)] and is affected by the demagnification (the Johann error), i.e., because the detector and the sample do not sit exactly on the Rowland circle of the analyzer [Fig. 3(a)]. The size of the detector aperture influences the degree to which these terms contribute as does the perfection of the analyzer.<sup>15</sup> The contribution due to demagnification can be kept small by employing analyzers of large bending radius (large focal distance). Focusing the incoming beam onto the sample

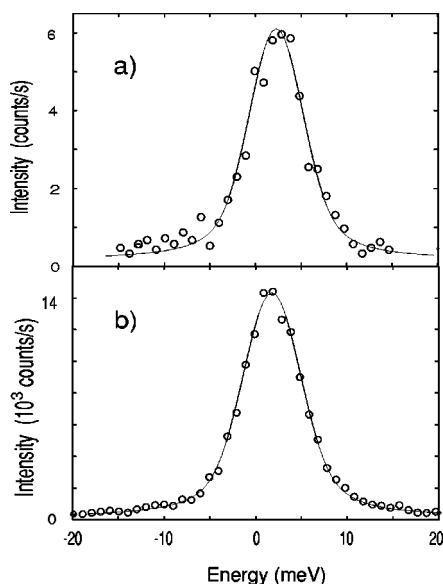


FIG. 4. Total energy resolution function of the monochromator and the analyzer measured using (a) a flat crystal, and (b) a focusing analyzer. The elastic scattering is from a Plexiglas, and the employed reflection was the Si(777).

minimizes the source size. Besides the detector pixel size, the block size preferably matches the acceptance angle of the reflection used at the specified angle  $\varepsilon$  away from backscattering. Choosing a large bending radius is a convenient method to reduce the geometrical contributions dominated by the first order term in Eq. (2) (Ref. 17).

The latest innovation in fabrication has yielded an analyzer with very good energy resolution and high reflectivity. To quantify the reflectivity we have done measurements using the Si(777) reflection. The elastic scattering from Plexiglas at  $8.5^\circ$  scattering angle [maximum of  $S(Q)$ ] was measured using a strain-free flat crystal at a distance of 3 m. The detector was positioned 0.6 mrad away from backscattering, which implies an acceptance angle of 0.6 mrad for the Si(777) reflection. The detector aperture was  $2 \times 2 \text{ mm}^2$ . This setup yielded a count rate of 6 counts/s for a flat (111) crystal positioned at 3 m distance [Fig. 4(a)]. The acceptance angle of 0.6 mrad implies a reflecting area of  $1.8 \times 1.8 \text{ mm}^2$ . But, the source size and the small aperture of the detector only permit the detection of x-rays from a reduced area of  $1.4 \times 1.4 \text{ mm}^2$ . Instead, with a focusing analyzer placed at a distance of 2.7 m, this area reduces further to  $1.1 \times 1.1 \text{ mm}^2$ . The block sizes of current analyzers sitting at a distance of 2.7 m cover an area of ca.  $0.9 \times 0.9 \text{ mm}^2$ , i.e., *the whole area of each block contributes to the reflectivity*. However, one loses 20% reflectivity in the 0.1 mm wide grooves. The exposed area of our analyzer is 83 mm in diameter, which encompasses 5411 blocks. Assuming all blocks are well aligned, we calculate an expected count rate with the focusing analyzer of  $21.7 \times 10^3 \text{ counts/s}$  ( $= (0.9/1.1)^2 \times 6 \text{ counts/s} \times 5411$ ). In fact, we measure a count rate of  $14.3 \times 10^3 \text{ counts/s}$  [Fig. 4(b)], which represents an analyzer efficiency of 66%. We note that this is a net gain provided by the analyzer of about 2400. The measured full width at half maximum (FWHM) of the analyzer focus of 2.6 mm was larger than the detector aperture and indicates the

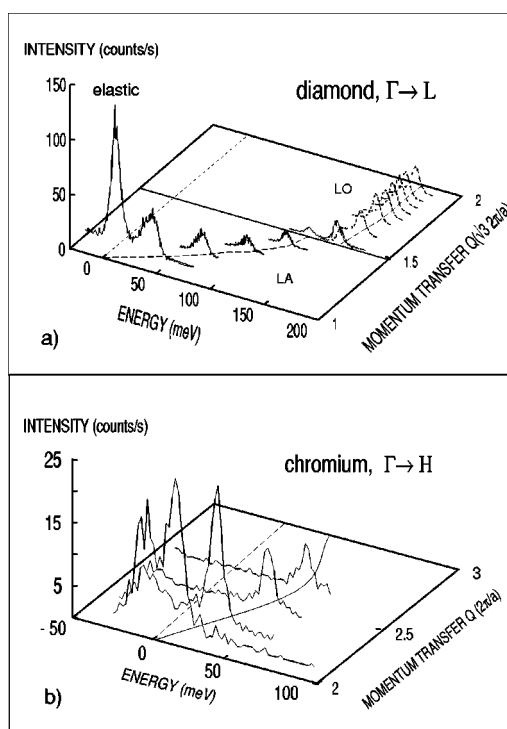


FIG. 5. Spectra at different momentum transfers representing longitudinal modes in diamond (a) and chromium (b).

presence of a slope error of about  $150 \mu\text{rad}$  (Ref. 15) (i.e., the mismatch of focus and detector aperture explains the 34% loss in the efficiency). Besides the high efficiency, the analyzer also performs with the same total energy resolution of 7.6 meV (FWHM) as was achieved with the flat crystal (Fig. 4). The profile of the energy resolution function is not purely Lorentzian. The line is the energy resolution calculated via ray tracing considering the intrinsic resolution of the Si(777) reflection, a block size of  $0.9 \text{ mm}^2$ , and a source size of  $0.5 \text{ mm}^2$ . During the reflectivity measurements, the flux of the monochromatized incident beam was  $3 \times 10^9 \text{ photons/s}$ . Finally, the use of a well-designed detector is essential to the efficiency and reliability of the instrument. The detector that we used is a CdZnTe detector specially adapted by Amptek Inc. The measured background was 0.03 counts/s at 14 keV.

To demonstrate the feasibility of our new instrument to study high frequency phonons, we measured longitudinal acoustical and optical phonons in diamond [Fig. 5(a)].<sup>18</sup> Our work on phonon scattering by (a high Z element) chromium yields intensities of 15 counts/s comparable with the intensities in diamond, i.e., the higher electron density compensates the loss due to absorption [Fig. 5(b)].

## ACKNOWLEDGMENTS

The authors are indebted to V. I. Kushnir for assistance and to SRI-CAT staff of sector 3 at the APS for the performance of the beamline. We are also indebted to the management of the APS, the Experimental Facilities Division, and the SRI-CAT for their support. Use of the APS was supported by the U.S. Department of Energy, Basic Energy Sci-

ences, Office of Energy Research, under Contract No. W-31-109-ENG-38, and the Division of Materials Sciences, under Contract No. DEFG02-96ER45439.

<sup>1</sup>E. Burkel, *Springer Tracts in Modern Physics* (Springer, Berlin, 1991), Vol. 125.

<sup>2</sup>B. Dorner, E. Burkel, and J. Peisl, *Nucl. Instrum. Methods Phys. Res. A* **426**, 450 (1986).

<sup>3</sup>E. Burkel, B. Dorner, and J. Peisl, *Europhys. Lett.* **3**, 957 (1987).

<sup>4</sup>R. Verbeni, F. Sette, M. H. Krisch, U. Bergmann, B. Gorges, C. Halcoussis, K. Martel, C. Masciovecchio, J. F. Ribois, G. Ruocco, and H. Sinn, *J. Synchrotron Radiat.* **3**, 62 (1996).

<sup>5</sup>B. Alefeld, M. Birr, and A. Heidemann, *Neutron Inelastic Scattering* (Int. Atomic Energy Agency, Vienna, 1968), p. 381.

<sup>6</sup>B. Sykora and L. Peisl, *Z. Angew. Phys.* **30**, 320 (1970).

<sup>7</sup>W. Graeff and G. Materlik, *Nucl. Instrum. Methods Phys. Res.* **195**, 97 (1982).

<sup>8</sup>T. S. Toellner, T. Mooney, S. Shastri, and E. E. Alp, *SPIE Proceedings Series* (Society of Photo-Optical Instrumentation Engineers, Bellingham, Washington, 1992), Vol. 1740, p. 218.

<sup>9</sup>W. Sturhahn, T. S. Toellner, E. E. Alp, X. W. Zhang, M. Ando, Y. Yoda, S. Kikuta, M. Seto, C. W. Kimball, and B. Dabrowski, *Phys. Rev. Lett.* **74**, 3832 (1995).

<sup>10</sup>L. Assoufid, K. W. Quast, and H. T. L. Nain, *SPIE Proceedings Series* (Society of Photo-Optical Instrumentation Engineers, Bellingham, Washington, 1996), Vol. 2855, p. 250.

<sup>11</sup>P. Fernandez, T. Graber, W.-K. Lee, D. M. Mills, C. S. Rogers, and L. Assoufid, *Nucl. Instrum. Methods Phys. Res. A* **400**, 476 (1997).

<sup>12</sup>T. Ishikawa, Y. Yoda, K. Izumi, C. K. Susuki, X. W. Zhang, M. Ando, and S. Kikuta, *Rev. Sci. Instrum.* **63**, 1015 (1992).

<sup>13</sup>A. T. Macrander, M. Schwoerer-Böhning, P. M. Abbamonte, and M. Hu, *SPIE Proceedings Series* (Society of Photo-Optical Instrumentation Engineers, Bellingham, WA, 1997), Vol. 3151, p. 271.

<sup>14</sup>M. Schwoerer-Böhning, P. M. Abbamonte, A. T. Macrander, and V. I. Kushnir, *SRI-CAT Newsletter* **3**, 2 (1997) <http://www.aps.anl.gov/xfd/www/xfd/sri-cat/nl>.

<sup>15</sup>R. Blasdel and A. T. Macrander, *Rev. Sci. Instrum.* **66**, 2075 (1995).

<sup>16</sup>M. Schwoerer-Böhning, P. M. Abbamonte, A. T. Macrander, and V. I. Kushnir, *SPIE Proceedings Series* (Society of Photo-Optical Instrumentation Engineers, Bellingham, Washington, 1997), Vol. 3151, p. 282.

<sup>17</sup>F. Sette, G. Ruocco, M. Krisch, U. Bergmann, C. Masciovecchio, V. Mazzacurati, G. Signorelli, and R. Verbeni, *Phys. Rev. Lett.* **75**, 850 (1995).

<sup>18</sup>M. Schwoerer-Böhning, A. T. Macrander, and D. A. Arms, *Phys. Rev. Lett.* **80**, 5572 (1998).